Dynamical density-density correlations in one-dimensional Mott insulators

Walter Stephan and Karlo Penc*
Max-Planck-Institut für Physik Komplexer Systeme, Bayreuther Strasse 40, D-01187 Dresden, Germany
(Received 11 September 1996)

The dynamical density-density correlation function is calculated for the one-dimensional, half-filled Hubbard model extended with nearest-neighbor repulsion using the Lánczos algorithm for finite-size systems and analytically for large on-site repulsion compared to hopping amplitudes. At the zone boundary an excitonic feature exists for any finite nearest-neighbor repulsion and exhausts most of the spectral weight, even for parameters where no exciton is visible at zero momentum. [S0163-1829(96)52048-5]

Materials such as $SrCuO_2$ and Sr_2CuO_3 are believed to be quite well described by the one-dimensional half-filled Hubbard model.[1] With the current level of experimental technology it is possible to measure dielectric response (which is directly related to the density response function) with good resolution in both momentum and energy transfer,[2,3] which makes it of great interest to understand the response expected from this simplest model of a Mott-Hubbard insulator. In this paper we present the combined results of analytic and numerical calculations, which clarify the nature of the dynamical density response function of the Hubbard model including also nearest-neighbor repulsion, which is a first step to the inclusion of the long-range Coulomb interaction. The results presented may serve as a indication of the appropriateness of the model to particular materials once experimental data become available. Previous work of Mori, Fukuyama, and Imada[4] in this direction was based on an effective low-energy model whose relation to our extended Hubbard model is nontrivial.

The extended Hubbard model is defined as

$$\mathcal{H}=-t\sum_{j,\sigma}\left(c^{\dagger}_{j+1,\sigma}c_{j,\sigma}+\text{H.c.}\right)+\mathcal{U}+\mathcal{V}, \tag{1}$$

where $\mathcal{U}=U\Sigma_j n_{j,\uparrow}n_{j,\downarrow}$ is the on-site Coulomb repulsion, $\mathcal{V}=V\Sigma_j n_j n_{j+1}$ is the nearest-neighbor repulsion and $n_i=n_{i\uparrow}+n_{i\downarrow}$ is the density at site i.

The imaginary part of the density-density correlation function is given by

$$\mathcal{N}(k,\omega)=\sum_f |\langle f|n_k|\text{GS}\rangle|^2\,\delta(\omega-E_f+E_{\text{GS}}), \tag{2}$$

where $|\text{GS}\rangle$ is the half-filled ground state and $|f\rangle$ denotes a final state with energy E_f and momentum $k=P_f$. Note that the optical conductivity is directly related to the density-density correlation function through the continuity equation (see, e.g., Ref. 5),

$$\text{Re}\sigma(\omega)=\lim_{k\to 0}\frac{\omega}{4\sin^2(k/2)}\mathcal{N}(k,\omega). \tag{3}$$

For the case of small charge gap compared to bandwidth $\sigma(\omega)$ has been calculated by Giamarchi and Millis[6] using bosonization, and the large U case was studied by Gebhard *et al.*[7]

We evaluate Eq. (2) by (a) direct diagonalization, which is limited to small clusters; (b) for $U\gg t,V$ we perform a canonical transformation of the type introduced by Harris and Lange[8] to get a ''tJ'' like effective model. This model is then diagonalized for larger system sizes; (c) finally, for the effective model in the thermodynamic limit an analytic expression is obtained using the factorized wave function of Ogata and Shiba.[9]

a. Exact diagonalization of Hubbard model. Using the standard Lánczos algorithm, it is straightforward to calculate $\mathcal{N}(k,\omega)$ for finite size clusters of L sites. In Fig. 1 we show a typical plot for relatively large U and intermediate V. There are several features to observe: the spectra consist of

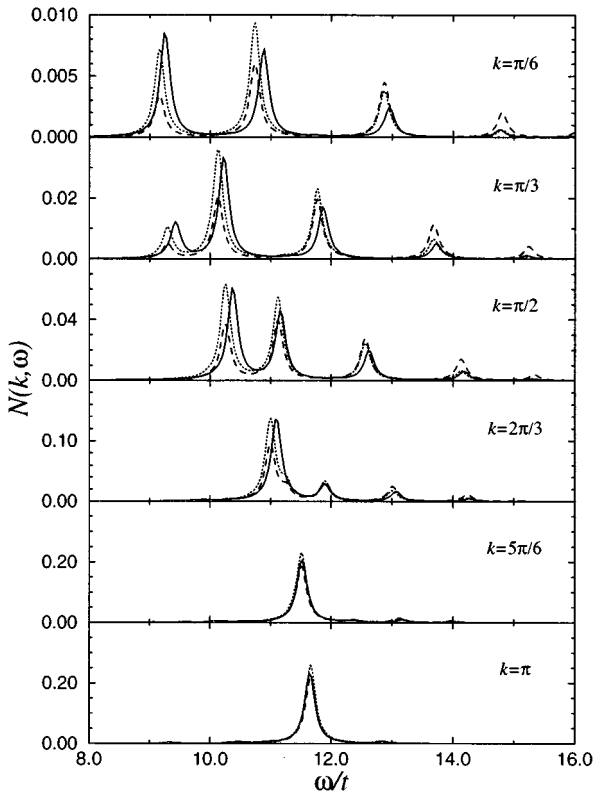

FIG. 1. $\mathcal{N}(k,\omega)$ of a half-filled twelve site Hubbard model (full line) for $V=t$, $U/t=12$, effective model with (dotted line) and without (dashed line) t^2/U^2 corrections in the density operators. The δ functions are plotted as Lorentzians of width $0.1t$.

dominant peaks which are distributed over a frequency range from approximately $U-V-4t$ to $U-V+4t$ at small momentum transfer, narrowing to a single peak near $U-V$ at the zone boundary. There are also less intense features which are barely visible in the figure whose weight increases slightly for smaller U. The number of large peaks at small momentum scales linearly with the system size, and is therefore most naturally interpreted as the finite-size precursor to a continuum absorption. Near the zone boundary, however, for all accessible system sizes we see only a single peak when V is finite. We shall see that this is due to the appearance of an exciton below the continuum. A further feature of $\mathcal{N}(k,\omega)$ is the asymmetry in the weight distribution: the spectra are skewed toward lower frequency, which is more pronounced for either smaller U or greater V. Our main interest here is the region $V \ll U$, however we note that for V approaching $U/2$ the transition to the charge density wave state[10] is directly seen as a drastic softening of the response at $k=\pi$. Apart from the features presented there is of course also the special case of $k=0$ where the response is simply a delta function at zero frequency.

b. Effective model. In order to understand more clearly the above observations it is instructive to derive an effective model in the strong-coupling large U limit. We closely follow the approach of Harris and Lange,[8] however, for details and notation we refer to Ref. 11. We first define

$$\widetilde{T}_0=\widetilde{\mathcal{V}}-t\sum_{i,\delta,\sigma}\widetilde{n}_{i,\bar{\sigma}}\widetilde{c}^{\dagger}_{i,\sigma}\widetilde{c}_{i+\delta,\sigma}\widetilde{n}_{i+\delta,\bar{\sigma}}$$

$$-t\sum_{i,\delta,\sigma}(1-\widetilde{n}_{i,\bar{\sigma}})\widetilde{c}^{\dagger}_{i,\sigma}\widetilde{c}_{i+\delta,\sigma}(1-\widetilde{n}_{i+\delta,\bar{\sigma}})$$

$$T_U=-t\sum_{i,\delta,\sigma}\widetilde{n}_{i,\bar{\sigma}}\widetilde{c}^{\dagger}_{i,\sigma}\widetilde{c}_{i+\delta,\sigma}(1-\widetilde{n}_{i+\delta,\bar{\sigma}}), \tag{4}$$

and $\widetilde{T}_{-U}=\widetilde{T}_U^{\dagger}$ where the subscript denotes the change in the eigenvalue of $\widetilde{\mathcal{U}}$ induced, corresponding to the change in the number of doubly occupied sites, so that

$$\mathcal{H}_{\rm eff}=\widetilde{\mathcal{U}}+\widetilde{T}_0+\frac{1}{U}[\widetilde{T}_U,\widetilde{T}_{-U}]+\mathcal{O}\left(\frac{t^3}{U^2},\frac{Vt^2}{U^2}\right). \tag{5}$$

Here by $\widetilde{O}$ we denote the canonically transformed operators. The expression for $\mathcal{H}_{\rm eff}$ at the operator level is quite long and complicated, here we rather give the effect of $U^{-1}[\widetilde{T}_U,\widetilde{T}_{-U}]$ applied to the basis states:

$$|\sigma\bar{\sigma}\rangle\rightarrow(2t^2/U)(|\bar{\sigma}\sigma\rangle-|\sigma\bar{\sigma}\rangle)$$

$$|\tau\bar{\tau}\rangle\rightarrow(2t^2/U)(|\tau\bar{\tau}\rangle+|\bar{\tau}\tau\rangle)$$

$$|\tau\sigma\bar{\sigma}\rangle\rightarrow(t^2/U)(|\bar{\sigma}\sigma\tau\rangle-|\sigma\bar{\sigma}\tau\rangle)$$

$$|\sigma\bar{\sigma}\tau\rangle\rightarrow(t^2/U)(|\tau\bar{\sigma}\sigma\rangle-|\tau\sigma\bar{\sigma}\rangle)$$

$$|\tau\bar{\tau}\sigma\rangle\rightarrow-(t^2/U)(|\sigma\tau\bar{\tau}\rangle+|\sigma\bar{\tau}\tau\rangle)$$

$$|\sigma\tau\bar{\tau}\rangle\rightarrow-(t^2/U)(|\tau\bar{\tau}\sigma\rangle+|\bar{\tau}\tau\sigma\rangle), \tag{6}$$

where σ stands for spins and τ for empty (e) or doubly occupied (d) states, and we use the convention where the creation operators for the states are ordered with increasing site index and in case of double occupancy we use $c^{\dagger}_{i\uparrow}c^{\dagger}_{i\downarrow}$.

In order to calculate the matrix elements describing the transition to the upper Hubbard band in Eq. (2), we must transform the electron density operator appropriately,[11] $\widetilde{n}_{i,U}=\widetilde{n}^{(1)}_{i,U}+\widetilde{n}^{(2)}_{i,U}+\cdots$, where the leading term $\widetilde{n}^{(1)}_{i,U}=[\widetilde{T}_U,\widetilde{n}_{i,0}]/U$ reads

$$\widetilde{n}^{(1)}_{i,U}=\frac{t}{U}\sum_{\delta=\pm1}[\widetilde{n}_{i\bar{\sigma}}\widetilde{c}^{\dagger}_{i\sigma}\widetilde{c}_{i+\delta\sigma}(1-\widetilde{n}_{i+\delta,\bar{\sigma}})$$

$$-\widetilde{n}_{i+\delta\bar{\sigma}}\widetilde{c}^{\dagger}_{i+\delta\sigma}\widetilde{c}_{i\sigma}(1-\widetilde{n}_{i,\bar{\sigma}})]. \tag{7}$$

The next order correction $\widetilde{n}^{(2)}$ will be considered later.

At half–filling the ground state wave function of $\mathcal{H}_{\rm eff}$ is simply that of the Heisenberg model, and matrix elements are with the states in the upper Hubbard band—i.e., with the states containing exactly one doubly occupied site. Then $\langle f|\widetilde{n}^{(1)}_{j,U}|{\rm GS}\rangle=t/U\langle f|\Sigma_{\sigma,\delta}(\widetilde{c}^{\dagger}_{j\sigma}\widetilde{c}_{j+\delta\sigma}-\widetilde{c}^{\dagger}_{j+\delta\sigma}\widetilde{c}_{j\sigma})|{\rm GS}\rangle$ holds and $\mathcal{N}(k,\omega)$ simplifies to

$$\mathcal{N}(k,\omega)=L\frac{t^2}{U^2}4\sin^2\frac{k}{2}\sum_f|\langle f|(\widetilde{c}^{\dagger}_{1\sigma}\widetilde{c}_{0\sigma}-\widetilde{c}^{\dagger}_{0\sigma}\widetilde{c}_{1\sigma})|{\rm GS}\rangle|^2$$

$$\times\delta(\omega-E_f+E_{\rm GS})\,\delta_{k,P_f}. \tag{8}$$

The density response for this effective model as determined by exact diagonalization is shown in Fig. 1 as the dashed curve. We can see that the overall behavior follows that of the Hubbard model, however, there are significant deviations in the distribution of weights near the edges of the spectrum for the not extremely large U used. This agreement may be improved by including also the next to leading order correction to the density operator:

$$\widetilde{n}^{(2)}_{j,U}=\frac{1}{U^2}[[\widetilde{T}_U,\widetilde{T}_0],\widetilde{n}_{j,0}]=\frac{t^2}{U^2}\sum_{\sigma,\delta}[(1-2\widetilde{n}_{j+\delta,\bar{\sigma}})$$

$$\times(\widetilde{c}^{\dagger}_{j+2\delta,\sigma}\widetilde{c}_{j,\sigma}-\widetilde{c}^{\dagger}_{j,\sigma}\widetilde{c}_{j+2\delta,\sigma})$$

$$+2(\widetilde{c}^{\dagger}_{j+2\delta,\bar{\sigma}}\widetilde{c}^{\dagger}_{j+\delta,\sigma}\widetilde{c}_{j+\delta,\bar{\sigma}}\widetilde{c}_{j,\sigma}$$

$$-\widetilde{c}^{\dagger}_{j,\bar{\sigma}}\widetilde{c}^{\dagger}_{j+\delta,\sigma}\widetilde{c}_{j+\delta,\bar{\sigma}}\widetilde{c}_{j+2\delta,\sigma})]$$

$$+\frac{tV}{U^2}\sum_{\sigma,\delta}(\widetilde{c}^{\dagger}_{j\sigma}\widetilde{c}_{j+\delta\sigma}-\widetilde{c}^{\dagger}_{j+\delta\sigma}\widetilde{c}_{j\sigma}), \tag{9}$$

where the final form is correct only when applied to a half-filled state with no double occupancy. The diagonalization result including also these terms in the matrix elements is shown as the dotted line in Fig. 1. The agreement with the Hubbard model results as compared to the first approximation is noticeably improved as regards the skewing of the spectrum.

c. Analytic approach. The operator $\widetilde{c}^{\dagger}_{1\sigma}\widetilde{c}_{0\sigma}-\widetilde{c}^{\dagger}_{0\sigma}\widetilde{c}_{1\sigma}$ in Eq. (8) removes a spin singlet from the Heisenberg wave function and an ed ''singlet'' is created:

$$|\downarrow\uparrow\cdots\rangle-|\uparrow\downarrow\cdots\rangle\rightarrow2(|de\cdots\rangle-|ed\cdots\rangle).$$

The wave function of the final state in the large-U limit can be written in the product form:[9]

$$|f\rangle=\hat{R}(|\psi\rangle\otimes|\chi\rangle\otimes|\varphi\rangle), \tag{10}$$

where $|\psi\rangle$ describes $L-2$ spinless free fermions on an L site lattice with twisted boundary condition[12] (the holes represent the e and d), $|\chi\rangle$ is the squeezed wave function of the remaining $L-2$ spins with momentum $Q=2\pi J/(L-2)$, $(J=0,\ldots,L-3)$ and $|\varphi\rangle=(|ed\rangle+|de\rangle)/\sqrt{2}$. The operator $\hat{R}=\Sigma_j e^{i\pi n_{j\uparrow}n_{j\downarrow}}$ corrects for the opposite sign of hopping of the d compared to e. Using this wave function, for $\mathcal{N}(\omega,k)$ we get

$$\mathcal{N}(k,\omega)=L\frac{t^2}{U^2}16\sin^2\frac{k}{2}\sum_{Q,I_1^h,I_2^h}F_Q B_{01}\delta(\omega-E_f+E_{\mathrm{GS}})\,\delta_{k,P_f}. \tag{11}$$

The spin part gives $F_Q=\Sigma|\langle\chi_Q^{L-2}|\hat{\mathcal{F}}|\chi_{\mathrm{GS}}^{L}\rangle|^2$, where the operator $\hat{\mathcal{F}}$ removes a singlet from the first two sites of the spin wave function and the sum is over all states with momentum Q. This has been studied in detail in Ref. 13, where it is found that $\approx$97% of the total weight, $\Sigma_Q F_Q=\langle\vec{S}_0\cdot\vec{S}_1+\frac{1}{4}\rangle$ ($\rightarrow$ln2 in the thermodynamic limit), is concentrated at $Q=0$. This remarkable feature makes the calculation simple.

The matrix element coming from the charge part of the wave function is $B_{01}=|\langle\psi_f|b_0 b_1|\psi_{\mathrm{GS}}\rangle|^2$, where b_i annihilates a spinless fermion. First, we discuss the case $V=0$. Then $|\psi\rangle$ can be characterized by the quantum numbers of the two holes, I_1^h and I_2^h, with momenta $Lk_{1,2}^h=2\pi I_{1,2}^h+Q$, and the momentum and energy are

$$P_f=-k_1^h-k_2^h+Q=\frac{2\pi}{L}(-I_1^h-I_2^h+J)$$

$$E_f=E_{\mathrm{GS}}+2t(\cos k_1^h+\cos k_2^h)+U, \tag{12}$$

where we have neglected the small energy difference between the exchange energies of the ground state and the final states of the order of t^2/U; furthermore we assume that the ground state has momentum 0 (i.e., the system has 2,6,10 etc. sites). Then B_{01} reads

$$B_{01}=\frac{4}{L^2}\sin^2\frac{k_1^h-k_2^h}{2}. \tag{13}$$

Let us next consider the case with finite V: The effect of the nearest-neighbor repulsion appears as attraction between the empty and double occupied sites, and leads to an extra $-V(1-n_j)(1-n_{j+1})$ term in the Hamiltonian describing the spinless fermions. Therefore we expect bound states (excitons) to appear in the spectrum. In the large-U limit the factorized wave function remains an eigenstate even introducing the V term,[7] supposing that $V\ll U$. The two particle problem can be solved using the standard Bethe-ansatz,

$$|\psi\rangle=\sum_{j_1<j_2}a_{j_1,j_2}|j_1,j_2\rangle, \tag{14}$$

where the holes are located at sites j_1 and j_2. Since the system is translationally invariant, we can separate the momentum of the holes K (so that the total momentum is $P_f=-K+Q$):

$$a_{j_1,j_2}=e^{i(j_1+j_2)K/2}[e^{iq(j_2-j_1)}+\nu e^{iq(L-j_2+j_1)}]. \tag{15}$$

From the twisted boundary condition $a_{0,j}=-e^{-iQ}a_{j,L}$ (we assume that the number of fermions and holes is even), $\nu=-e^{i(KL/2-Q)}=\pm1$, and the quantization $LK=2\pi I_K+2Q$ follow, where I_K is an integer. Then the energy is simply (we introduce for compactness $E'=E-U$ and $\omega'=\omega-U$):

$$E'=4t\cos\frac{K}{2}\cos q, \tag{16}$$

and the secular equation for q becomes

$$2\pi I=Lq+2\arctan\frac{V\cos q+2t\cos(K/2)}{V\sin q}, \tag{17}$$

where for $\nu=1$ the quantum number I is integer, $I=0,1,\ldots,L/2-1$, and half odd integer $[I=\frac{1}{2},\frac{3}{2},\ldots,(L-3)/2]$ for $\nu=-1$. Depending on the ratio $V/[2t\cos(K/2)]$, we can have either all the q's real, or, for sufficiently large ratio a bound state can appear with complex q. In the thermodynamic limit, $L\rightarrow\infty$, the bound state is formed for $V>2t\cos K/2$ with energy

$$E'_{\mathrm{exc}}=-V-\frac{4t^2}{V}\cos^2\frac{K}{2}. \tag{18}$$

B_{01} is now given by $|a_{0,1}|^2/\Sigma_{j_1<j_2}|a_{j_1,j_2}|^2$ and, after a straightforward but tedious calculation, it reads

$$B_{01}=\frac{1}{L}\frac{16t^2\cos^2\frac{K}{2}-E'^2}{L\left(4t^2\cos^2\frac{K}{2}+VE'+V^2\right)-VE'-2V^2}. \tag{19}$$

At this point we have the weights to leading order in t/U. We have performed analogous calculations including also the term $\tilde{n}^{(2)}$ in the matrix elements, and the result obtained will be given later. Note that there are also contributions of the same order coming from the wave function correction, which would require going beyond the factorized wave function. In order to investigate the relevance of these terms, we present in Fig. 2 a comparison of different approximations. Apart from an energy shift $\mathcal{O}(t^2/U)$ the dashed line is seen to be quite reliable, and is in fact better as far as the distribution of weights is concerned than is the dotted line, which shows that the operator corrections are more significant than those to the wave function.

In the continuum limit we introduce $g(K,\omega')=L\Sigma_I B_{01}\delta(\omega'-E'_f)$, and we get

$$g(K,\omega')=\frac{1}{2\pi}\frac{\sqrt{16t^2\cos^2\frac{K}{2}-\omega'^2}}{4t^2\cos^2\frac{K}{2}+V\omega'+V^2}\Theta\left(4t\cos\frac{K}{2}-|\omega'|\right)$$

$$+\left(1-\frac{4t^2}{V^2}\cos^2\frac{K}{2}\right)\delta(\omega'-E'_{\mathrm{exc}}), \tag{20}$$

$\int g(k,\omega)d\omega=1$, and $\mathcal{N}(k,\omega)$ now reads

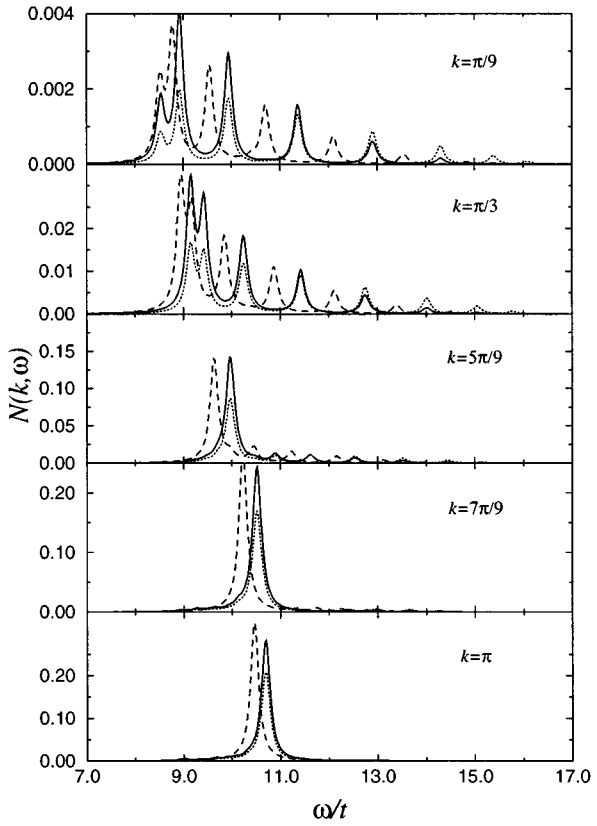

FIG. 2. $\mathcal{N}(k,\omega)$ for an 18-site cluster with $U=12t$ and $V=2t$. The solid line is the ''best'' strong-coupling limit result, where the exact wave functions and energies from the diagonalization of $\mathcal{H}_{\text{eff}}$ as well as the $\tilde{n}^{(2)}$ correction is included, which are, however, omitted for the dotted line. The dashed line includes $\tilde{n}^{(2)}$ but uses the leading order wave functions and energies for the final states.

$$\mathcal{N}(k,\omega)\approx\frac{t^2}{U^2}16\sin^2\frac{k}{2}F_0 g(k,\omega-U)+\mathcal{N}_{\text{inc}}(k,\omega), \quad (21)$$

where $\mathcal{N}_{\text{inc}}(k,\omega)$ contains the contributions from $Q\neq 0$ and its weight is small (3%) compared to the main features given by the $Q=0$ part.

The function $g(k,\omega)$ is shown in Fig. 3. As previously alluded to, the spectrum consists of both continuum and sharp excitonic features. For $V\approx t$ the exciton emerges from the continuum in the middle of the zone, and accounts for almost all of the spectral weight close to the zone boundary.

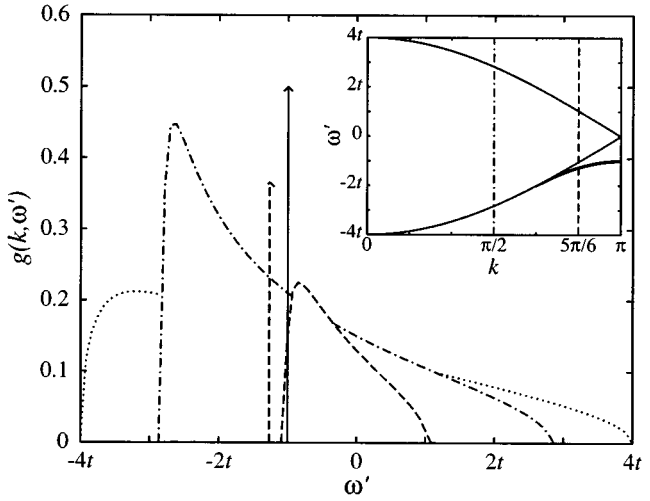

FIG. 3. $g(k,\omega')$ for $V=t$ and $k=0$ (dotted), $\pi/2$ (dashed dotted), $5\pi/6$ (dashed), and π (solid line). The weight of the excitonic peak is not in the same scale as the continuum. The inset shows the momentum dependence of the boundary, the continuum, and the exciton dispersion (heavy line).

For small momentum where the exciton is ''inside'' the continuum its presence may still be seen as a strong enhancement of the intensity of the spectrum near the lower edge. Of course for $V>2t$ the exciton is present for all momenta.

The effect of including $\tilde{n}^{(2)}$ in the operators can be given conveniently as

$$g(k,\omega)\rightarrow g(k,\omega)\left(1-\frac{4\omega+2V}{U}\right) \quad (22)$$

for the most important case of $Q=0$. For $V=0$, the t^3U^{-3} corrections only redistribute the weight and the sum rule $\int\mathcal{N}(k,\omega)d\omega=16\ln 2(t/U)^2\sin^2 k/2+\mathcal{O}(t^4/U^4)$ is satisfied.

To conclude, we have determined the density response of a simple model for a correlated quasi-one-dimensional insulator. The most surprising result is that excitons may appear near the zone boundary even if they are not present in the optical absorption (the $k\rightarrow 0$ limit), depending on the parameters chosen. It would be interesting if these features can be observed experimentally.

We acknowledge useful discussions with J. Fink, F. Gebhard, T. Giamarchi, and P. Horsch.

*On leave from the Research Institute for Solid State Physics, Budapest, Hungary.

[1] N. Motoyama, H. Eisaki, and S. Uchida, Phys. Rev. Lett. **76**, 3212 (1996), and references therein.

[2] Y. Y. Wang *et al.*, Phys. Rev. Lett. **77**, 1809 (1996); for a review on electron energy loss spectroscopy, see J. Fink, Adv. Electron. Electron Phys. **75**, 121 (1989).

[3] E. D. Isaacs *et al.*, Phys. Rev. Lett. **76**, 4211 (1996).

[4] M. Mori, H. Fukuyama, and M. Imada, J. Phys. Soc. Jpn. **63**, 1639 (1994).

[5] S. Nakajima, Y. Toyozawa, and R. Abe, *The Physics of Elementary Excitations* (Springer-Verlag, Berlin, 1980), Chap. 2.

[6] T. Giamarchi and A. J. Millis, Phys. Rev. B **46**, 9325 (1992).

[7] F. Gebhard *et al.*, Phil. Mag. B **75**, 47 (1997).

[8] A. B. Harris and R. V. Lange, Phys. Rev. **157**, 295 (1967).

[9] F. Woynarovich, J. Phys. C **15**, 97 (1982); M. Ogata and H. Shiba, Phys. Rev. B **41**, 2326 (1990).

[10] R. A. Bari, Phys. Rev. B **3**, 2662 (1971).

[11] H. Eskes and A. M. Oleś, Phys. Rev. Lett. **73**, 1279 (1994); H. Eskes, A. M. Oleś, M. B. J. Meinders, and W. Stephan, Phys. Rev. B **50**, 17 980 (1994).

[12] S. Sorella and A. Parola, J. Phys. Condens. Matter. **4**, 3589 (1992); K. Penc, F. Mila, and H. Shiba, Phys. Rev. Lett. **75**, 894 (1995).

[13] J. C. Talstra, S. P. Strong, and P. W. Anderson, Phys. Rev. Lett. **74**, 5256 (1995).